

# The Losses of Inverters and Off-Grid Photovoltaic Power Plants Efficiency Nexus Evaluation in Iraqi Region

Waleed Mohammed Khazaal<sup>1</sup>, Shaymaa Abed Hussein<sup>2</sup>, Majeed M. Abid<sup>3</sup>, Ann Samari Ibrahim<sup>4</sup>, Kadhum Al-Majdi<sup>5</sup>, Ahmed Read Al-Tameemi<sup>6</sup>, Hasan Ali Dhahi<sup>7</sup>

<sup>1</sup>*Department of biomedical engineering/ Mazaya university college Iraq*

<sup>2</sup>*Department of biomedical engineering/ Al-Manara College For Medical Sciences/ (Maysan)/Iraq*

<sup>3</sup>*Department of biomedical engineering/ Al-Hadi University College, Baghdad, 10011, Iraq.*

<sup>4</sup>*College of Engineering, Al-Esraa University/Baghdad, Iraq*

<sup>5</sup>*Department of biomedical engineering/ Ashur University College/Baghdad/ Iraq*

<sup>6</sup>*Department of biomedical engineering/ AL-Nisour University College/ Baghdad/ Iraq*

<sup>7</sup>*Department of biomedical engineering/ National University of Science and Technology, Dhi Qar, Iraq*

Given Iraq's significant radiation capacity, extensive geographical reach, and diverse climatic conditions, this research has opted to identify cities within Iraq that are well-suited for the establishment of solar power plants. The objective of this study is to conduct a quantitative evaluation of the influence of environmental variables on saturation losses and inverter efficiency in various geographical areas. The evaluation has been carried out. The study conducted a simulation to investigate the effects of several climatic and technical variables on the losses of the inverter, power production of the power plant, and capacity factor. The primary emphasis was placed on the examination of the impact stemming from the conversion ratio of the inverter, specifically in relation to the conversion from direct current (DC) to alternating current (AC). As the number of inverters increases, the DC to AC conversion ratio decreases from 1.21 to 1.06. Consequently, the saturation losses of the inverter notably decrease across all regions of the province, with a significant reduction of approximately 60%. Meanwhile, the potential for substantial improvements in the production capacity of solar farms. Notably, the Al-Risalah Photovoltaic Power Plant is expected to witness a 2.5% increase in production capacity compared to its previous performance.

**Keywords:** Photovoltaic Power Plants, Evaluation, Inverters, Solar Energy, Saturation losses.

## **1. Introduction**

The expansion of research and technology aimed at replacing non-renewable resources and polluting fossil fuels has been driven by growing energy demand and the imperative to protect the environment[1-3]. Presently, fossil fuels are the predominant source of energy in global energy networks. Nevertheless, it should be noted that these particular fuels are not recyclable and have the direct consequence of introducing greenhouse gases into the atmosphere[4-6]. This scenario gives rise to the consequences of significant environmental pollution, particularly with regard to the public health of the community. Moreover, volatility in the fossil fuel market's pricing has significant implications for both energy prices and security[7, 8].

In the present scenario, numerous nations around the globe are confronted with energy-related predicaments and have implemented diverse strategies to ensure the provision of sustainable and environmentally friendly energy sources. One of the recommended strategies in this domain involves the substitution of fossil fuels with renewable energy sources, including but not limited to hydropower, solar power, wind power, biomass, and geothermal energy. The adoption of renewable energy sources not only contributes to the mitigation of greenhouse gas emissions but also yields substantial economic advantages[9-13]. According to projections, it is anticipated that renewable energies might potentially account for about 34% of the global energy demand by the year 2040, establishing themselves as the predominant energy source in societies worldwide[14-16].

Solar energy is widely embraced globally due to its significant role and substantial impact as a prominent and influential form of renewable energy. Solar energy harnesses the radiant light and thermal energy emitted by the sun. Given its environmentally friendly attributes, comparatively affordable price, and inexhaustible supply, it has been suggested as a viable substitute for fossil fuels[17, 18].

One notable characteristic of solar energy is its widespread availability across many regions globally. Solar energy is readily accessible in a wide range of environments, spanning from arid and warm locations to frigid and moist ones. This characteristic renders solar energy an exceptionally versatile and ubiquitous source of energy[19, 20].

In recent years, solar energy has exhibited a greater growth rate compared to other forms of renewable energy, positioning it as one of the most rapidly expanding sources within the renewable energy sector. The deployment of photovoltaic systems, which harness solar energy to produce electrical power, is experiencing a substantial growth rate. This particular form of energy generation, being both reliable and adaptable, minimizes environmental harm and demonstrates economic viability[21-25].

According to market analysts, it is anticipated that the deployment of photovoltaic systems will witness substantial growth by the year 2050, thereby potentially contributing up to 25% of the total energy output required by civilization. The shifts in perspectives about energy production and use not only contribute to environmental enhancement but also yield economic benefits by bolstering productivity and sustainability inside communities while simultaneously mitigating reliance on fossil fuels[26-30].

The primary utilization of solar energy systems lies in their role as an energy source

integrated with the power grid. Additional applications of solar energy encompass the utilization of solar water pumps, the integration of solar energy in telecommunication towers, as well as its incorporation in microgrids and smart grids[31-33].

As previously said, renewable energies, particularly solar energy, have become increasingly prominent within the energy portfolios of both developed and developing nations. Iraq presents a favorable investment opportunity for photovoltaic energy due to its advantageous geographical location and an annual average of 300 days of abundant sunshine. The province of Baghdad is recognized as one of the leading provinces in terms of its potential for solar energy production, ranking within the top five provinces. Given the substantial expenses associated with solar power plants, enhancing the efficiency of these facilities becomes of paramount significance. The efficiency of the inverter employed in a solar power plant is a significant determinant of its overall power output. This paper evaluates the impact of inverter performance on the efficiency of a solar power plant in the cities of Baghdad province, taking into account the influence of power plant installation location. In order to achieve the intended objective, a photovoltaic power plant with a capacity of 10 megawatts has been specifically designed for the cities within the province of Baghdad. This design takes into consideration several factors, such as the geographic location, the utilization of the System Advisor model, and the meteorological data. The effect simulation takes into account many aspects that can impact the operation of photovoltaic farms. These elements include wind speed, elevation, radiation levels, ambient temperature, losses caused by photovoltaic modules, diode losses, losses from direct current and alternating current transmission lines, losses owing to shadows, and inverter losses. This study examines the impact of saturation losses in the inverter on the overall efficiency of a power plant through the utilization of simulation techniques.

#### Photovoltaic power plant; Modeling

Under standard conditions, photovoltaic panels have the capability to generate power at their rated capacity. Standard conditions refer to a set of predefined circumstances that are commonly used as a reference in solar energy research and analysis. These settings encompass a solar radiation intensity of 1 kW/m<sup>2</sup>, an ambient temperature of 25 degrees Celsius, and an air mass value of 1.5 AM. However, in practical applications, solar cells exhibit limited performance in ordinary settings and are subject to the influence of multiple factors. The expression for the maximum power of the panel is determined by equation 1[34].

$$P_{\max} = FF \times I_{sc}(G) \times V_{oc}(T_c) \quad (1)$$

where  $P_{\max}$  is the maximum power, the cell can produce. The short-circuit current in the radiation is denoted as  $I_{sc}(G)$ , while the open-circuit voltage of the cell at the cell temperature is represented as  $V_{oc}(T_c)$ . The accumulation factor (FF), which is utilized to assess the efficiency of the solar cell, is also referred to as the performance determinant. The values of  $I_{sc}(G)$  and  $V_{oc}(T_c)$  are determined by utilizing equation 2, and subsequently, the calculation of equation 3 is performed.

$$I_{sc}(G) = I_{sc,STC} \times \frac{G}{G_{STC}} \times (1 + \alpha(T_c - T_{STC})) \quad (2)$$

$$V_{oc}(T_c) = V_{oc,STC} \times (1 + \beta(T_c - T_{STC})) \times \left[ \ln \left( \frac{G}{C_0} + 1 \right) \times C_V - C_R \times G \right] \quad (3)$$

The variables  $G$  and  $G_{STC}$  are used in the equations above.  $G$  stands for solar radiation, and  $G_{STC}$  is the amount of radiation that normally happens, with a value of 1000 watts per square meter. The terms  $I_{SC,STC}$  and  $V_{oc,STC}$  refer to the short circuit current and open circuit voltage, respectively, of the module while it is operating under ordinary conditions. The variable  $T_c$  represents the temperature of the cell, while  $T_{STC}$  denotes the temperature under standard conditions, which is specifically defined as 25 degrees Celsius. Furthermore,  $\alpha$  represents the current reduction coefficient, whereas  $\beta$  denotes the voltage drop coefficient resulting from an increase in temperature. The correction coefficients of the voltage equation, namely  $C_R$ ,  $C_V$ , and  $C_G$ , are assigned values of  $2.514 \times 10^{-3}$ ,  $8.93 \times 10^{-2}$ , and  $1.088 \times 10^{-4} \text{ w/m}^2$ , respectively.

In order to determine the temperature of the cell, it is necessary to initially compute the temperature situated behind the module screen. This calculation is based on equation 4, which takes into account the solar radiation as well as the coefficients  $a$  and  $b$  associated with the ambient temperature and wind speed[35].

$$T_{Back} = G \cdot e^{a+b \cdot V_{wind}} + T_{Ambient} \quad (4)$$

The variables in question are  $T_{Ambient}$ ,  $V_{wind}$ ,  $G$ , coefficient  $a$ , and coefficient  $b$ .  $T_{Ambient}$  represents the ambient temperature,  $V_{wind}$  represents the wind speed, and  $G$  represents the solar radiation. Coefficient  $a$  denotes the upper limit of the module temperature, which is determined under conditions of low wind speed and high solar radiation levels. On the other hand, coefficient  $b$  signifies the rate at which the temperature of the photovoltaic module decreases as the wind speed increases. The calculation of the cell temperature  $T_c$  is performed by utilizing equation 5, which takes into account the temperature at the rear of the solar radiation module and the change in temperature  $dT$ .

$$T_c = T_{Back} + (G/G_{STC}) \times dT \quad (5)$$

In this case,  $T_{Back}$  is the temperature behind the module screen, and  $dT$  is the difference in temperature between the cell and the back surface of the module when a reference radiation of  $1000 \text{ w/m}^2$  is present. Furthermore, the FF denoted in equation 1 possesses a constant value for every individual cell and is computed in accordance with equation 6.

$$FF = \frac{V_{mp} \times I_{mp}}{V_{oc,STC} \times I_{sc,STC}} \quad (6)$$

Equation 6 denotes the variables  $V_{mp}$  and  $I_{mp}$ , which represent the maximum voltage and maximum current, respectively, at the point of maximum output power. Similarly,  $V_{oc,STC}$  and  $I_{sc,STC}$  correspond to the open circuit voltage and short circuit current, respectively, under standard conditions. Typically, the efficiency of silicon solar cells ranges from 70% to 75% in terms of the accumulation factor. When the radiation  $G$  is not orthogonal to the surface of the photovoltaic module (i.e., when the radiation angle on the module surface is not zero), the magnitude of the radiation varies depending on the radiation angle. This variation may be determined using equation 7.

$$G' = G \times \cos(\theta) \tag{7}$$

Thus, if the angle of radiation on the module's surface is not zero, G' is the amount of radiation on that surface. The symbol  $\theta$  represents the angle formed between a ray originating from the sun and a line that is perpendicular to the surface of the solar panel. The calculation of the radiation angle can be determined by employing equation 8.

$$\cos \theta = \cos \beta \cos \theta_z + \sin \beta \sin \theta_z \cos(\gamma_s - \gamma) \tag{8}$$

In the given context,  $\beta$  represents the inclination of the panel plane with respect to the earth's surface,  $\gamma$  denotes the orientation angle of the panel in relation to the south axis,  $\theta_z$  signifies the lateral angle, and  $\gamma_s$  represents the azimuth angle of the sun. The variable  $\gamma_s$  is quantified with respect to the southern direction, exhibiting negative values throughout both the afternoon and morning periods. The calculation of the angle of the sun side is determined using equation 9.

$$\cos \theta_z = \sin \delta \sin \phi + \cos \delta \cos \phi \cos \omega \tag{9}$$

The declination angle is shown by the symbol  $\delta$ , the latitude is represented by the symbol  $\phi$ , and the hour angle is denoted by the symbol  $\omega$ . Equation 10 is utilized to calculate the deviation angle, while equation 11 is employed to get the hour angle.

$$\delta = 23.45 \frac{\pi}{180} \sin \left( 2\pi \left( \frac{284+n}{365.25} \right) \right) \tag{10}$$

$$\sin \omega = \frac{\sin \alpha - \sin \delta \cdot \sin \phi}{\cos \delta \cdot \cos \phi} \tag{11}$$

The variable  $\alpha$  represents the angle of the sun's elevation, while the variable n denotes the day number in the Gregorian calendar. The value of n corresponds to February 1st. In the context of photovoltaic installations featuring multiple columns of solar arrays, it is possible to generate two distinct shadow models on the panels. In the initial iteration of the model, the width of the arrays W is comparatively smaller than the spacing between the columns of the arrays  $C_w$ , resulting in the potential formation of shadows on only one side of the array. In the scenario where both the slope of the plates and the installation angle align with the south, the resulting shadow will assume a rectangular shape. The dimensions of the shadow generated in this scenario are determined using equations 12 and 13.

$$W_s = W - (D + A \cos \beta) \times \frac{\sin \beta |\sin(\gamma_s - \gamma_c)|}{\tan \alpha \cdot \cos \beta + \sin \beta \cdot \cos(\gamma_s - \gamma_c)} \tag{12}$$

$$H_s = A \left\{ 1 - \frac{D + A \cos \beta}{\left( \frac{A \sin \beta \cdot \cos(\gamma_s - \gamma_c)}{\tan \alpha} + A \cos \beta \right)} \right\} \tag{13}$$

The transverse and longitudinal angles of the sun in the sky are denoted as  $\gamma_s$  and  $\alpha$ , respectively.  $\gamma_c$  represents the installation angle of the plates with regard to the connecting line between the two poles. Furthermore, the variable D represents the distance separating the arrays, whereas  $\beta$  denotes the slope at which they are installed. The variables W and A

represent the length and width of the arrays, whereas the variables  $W_s$  and  $H_s$  represent the length and width of the generated shadow, respectively.

In the second model, the breadth of the arrays  $W$  exceeds the inter-column spacing of the arrays  $C_w$ . In this scenario, the close proximity of the columns in the arrays gives rise to the potential occurrence of shadowing on both sides of the rear array. The arrays in the front row of the column as well as the adjacent columns of the array are what create this shadow model. In this particular scenario, the heights of the shadows generated on either side of the array exhibit equality and are determined through the utilization of equation 13. The calculation of the width of the shadow positioned on the side opposite to the sun's position in the sky with respect to local noon is determined using equation 12. Equation 14 yields the width of the shadow the sun casts in the sky ( $W'_s$ ).

$$W'_s = \frac{(D + A \cos \beta) \sin \beta |\sin(\gamma_s - \gamma_c)|}{\tan \alpha \cdot \cos \beta + \sin \beta \cdot \cos(\gamma_s - \gamma_c)} - C_\pi \quad (14)$$

The output power of the panel will decrease based on the type and intensity of the shadow cast on the bridge.

A device called an inverter changes the direct current (DC) power that the panels produce into alternating current (AC) power. This makes it easier to send to the end user. Equation (15) can be used to figure out the inverter's conversion ratio of direct current (DC) to alternating current (AC)[36].

$$\text{DC to AC conversion ratio} = \left( \frac{\text{The total DC power generated by the panels}}{\text{The total nominal capacity of AC inverters}} \right) \times 100 \quad (15)$$

The calculation of the power plant capacity coefficient, which assesses the efficiency of the solar power plant based on its yearly net energy production and photovoltaic power plant capacity, is performed using equation 16.

$$\text{Capacity factor} = \frac{\text{Annual net energy}}{\text{Power plant capacity}} \quad (16)$$

Photovoltaic power plant; simulation

The research employed the sophisticated functionalities of System Advisor Model (SAM) and Meteonorm software to model a 10-megawatt solar farm in different locations within the Baghdad governorate.

The program known as SAM provides accurate and pragmatic solutions for the design and analysis of various types of renewable energy systems, such as photovoltaic, wind, biomass, geothermal, and solar water heaters. The software lets users simulate different types of solar modules, such as monocrystalline and polycrystalline modules, as well as different types of inverters, which makes it more flexible. It is worth mentioning that SAM allows for the manual inclusion of particular modules or inverters in cases where they are not already included in the program. The System Advisor Model (SAM) simulates many things, such as shadows, wind speeds, radiation levels, altitude, snow accumulation, ambient temperature, diode and connection losses, DC and AC wiring losses, inverter power consumption,

nocturnal inverter consumption, losses caused by pollution and dust, and efficiency impacts from panels that aren't lined up correctly. The Meteonorm program is widely recognized as a robust and dependable tool for generating climate data pertaining to various geographical areas. The Meteonorm possesses data from 8350 meteorological stations located in various places, together with information regarding the quantity of satellites. It is important to acknowledge that the density of weather stations utilized by this program in Iraq and its bordering nations is significantly high and deemed favorable. One of the notable attributes of Meteonorm is its online information component, which offers users access to up-to-date meteorological data pertaining to their preferred environment. Additionally, users will have the capability to access and analyze the historical data pertaining to a certain geographic region across different time periods. The app offers users weather information across several time intervals, including minutes, hours, days, and months. The characteristics pertaining to the panel utilized are provided in Table 1.

Table 1. Specifications of the photovoltaic module used.

<u>Specification</u>	<u>Amount</u>
Nominal efficiency	20.57%
Maximum power	444.680 wdc
$V_{mp}$	77.7 vdc
$I_{mp}$	5.8 Adc
$V_{OC}$	90 vdc
$I_{SC}$	6.2 Adc
Operating temperature	44
Module area	2.168 m <sup>2</sup>
Number of cells	128

### Simulation results

Initially, a total of seven inverters are taken into account for the purpose of converting the direct current (DC) power generated by the panels into alternating current (AC) power. Consequently, based on the combined rated capacity of the panels and inverters, the ratio of DC to AC conversion is determined to be 1.21. For the given conversion ratio, Figures 1 and 2 show the solar power plant's output AC power and its capacity factor in different parts of Baghdad province. Furthermore, Figure 3 illustrates the losses incurred as a result of the shadow. According to the data presented in Figure 3, it can be observed that the Al-Rashid region exhibits the highest level of shadow loss, while the Baghdad region experiences the lowest level of shadow loss. The magnitude of shadow losses in the al-Rashid area exceeds that of the shadow losses seen in the Baghdad region by approximately 14%. It is evident that as one moves further away from the equator, the angle of the sun's radiation will become more oblique, resulting in a greater increase in shadow losses.

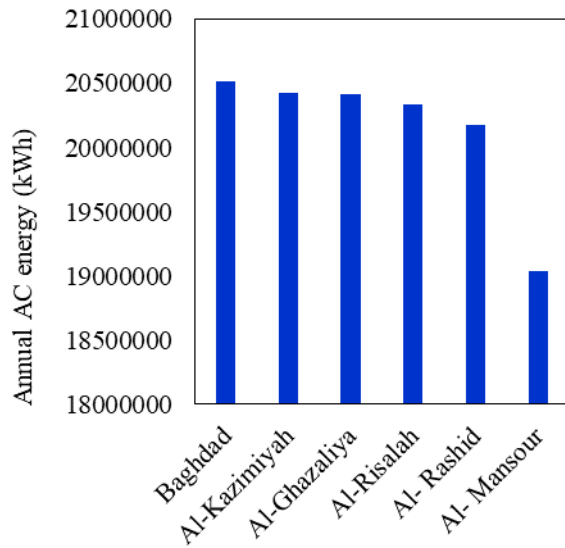


Fig. 1. AC energy produced by photovoltaic power plant in one year.

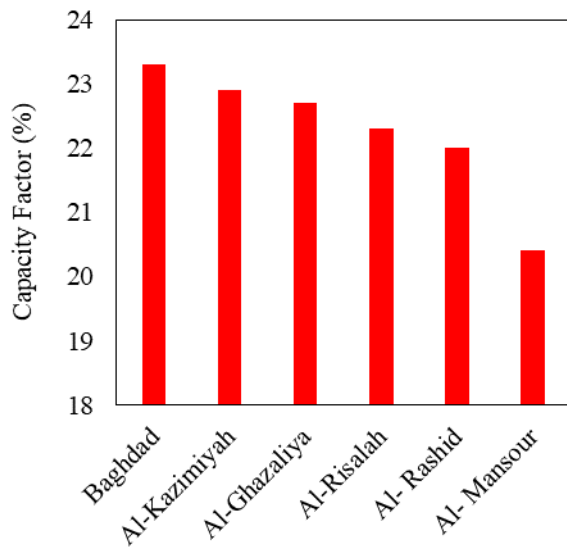


Fig.2.The capacity of the photovoltaic power plant.

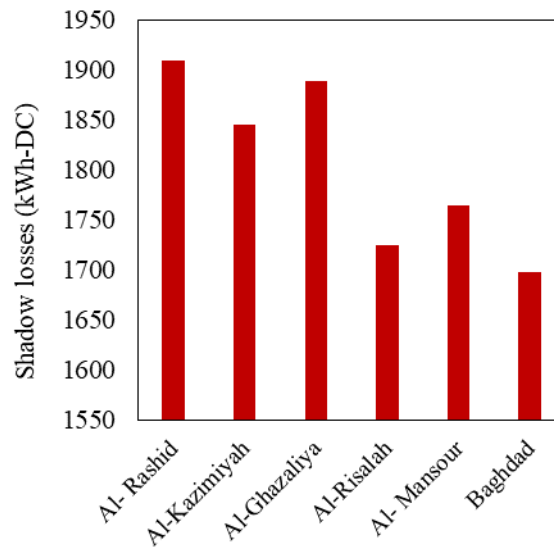


Fig.3.Shadow losses in photovoltaic power plant during one year.

The photovoltaic farm experiences additional losses, including inefficiencies in the inverter and losses due to inverter saturation. Due to the inverter's imperfect efficiency, the arrays inside the inverter lose some of the DC power they produce. Figure 4 illustrates the variations in inverter efficiency loss across different regions. When the photovoltaic (PV) array's generated direct current (DC) power exceeds the inverter's maximum input DC power threshold, inverter saturation losses become apparent. The inverter modulates the DC voltage in order to decrease the DC power in accordance with these circumstances. Increasing the voltage past the maximum power point (MPP) value accomplishes this by reducing direct current (DC), which in turn causes a decline in power output from its ideal state. Figure 5 illustrates the saturation losses incurred by the inverter at various locations.

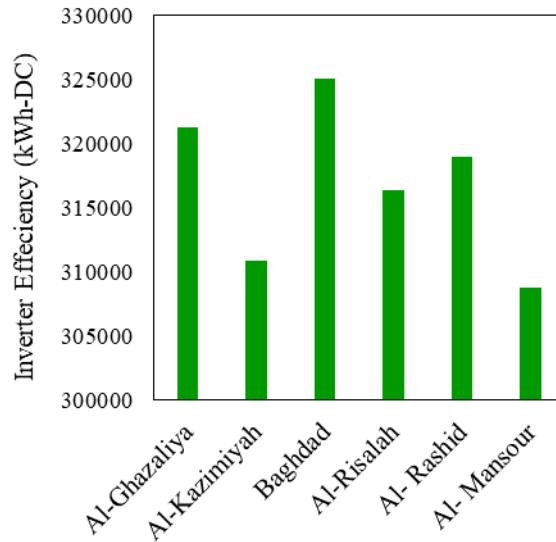


Fig.4.The rate of loss of efficiency in the period of one year.

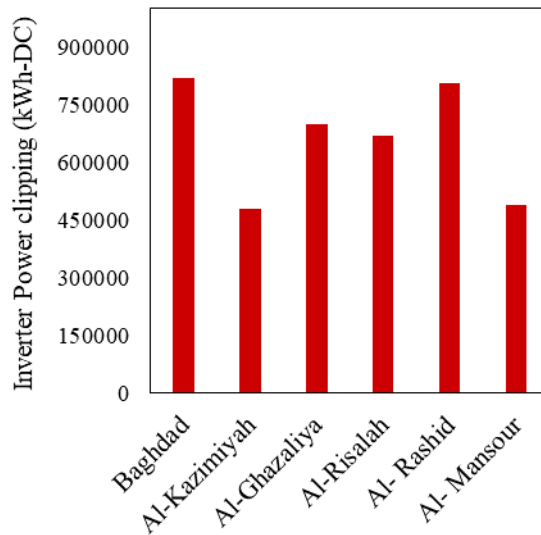


Fig.5.The amount of saturation losses of the inverter during one year.

According to the results shown in Figure 5, the inverter saturation loss goes up significantly when the DC to AC conversion ratio reaches 1.21. This is true across a number of regions. Consequently, the productivity of these regions experiences a substantial decline. In order to examine the impact of inverter saturation losses on the operational efficiency of the solar power plant, the quantity of inverters has been increased to a total of eight. Consequently, the ratio of direct current (DC) to alternating current (AC) conversion has been established at

1.06. The figures (6) and (7) depict the production power and capacity factor of solar fields in this particular scenario.

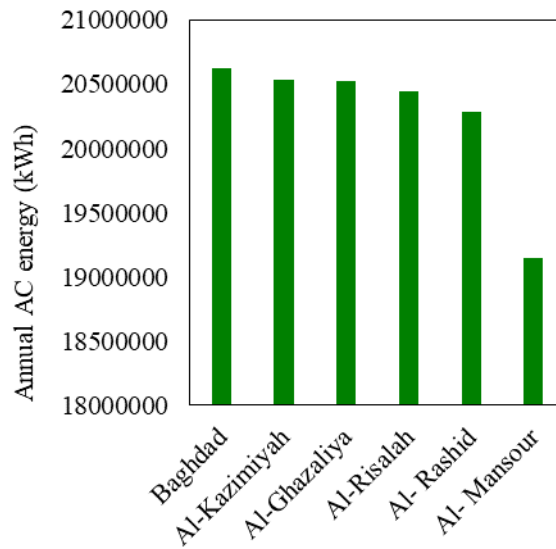


Fig. 6. AC energy produced by photovoltaic power plant in one year.

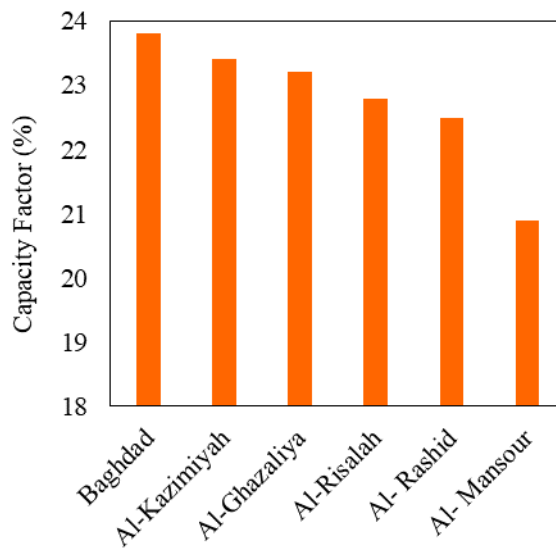


Fig. 7. The capacity of the photovoltaic power plant.

Figure 8 illustrates the quantification of inverter saturation losses within solar fields.

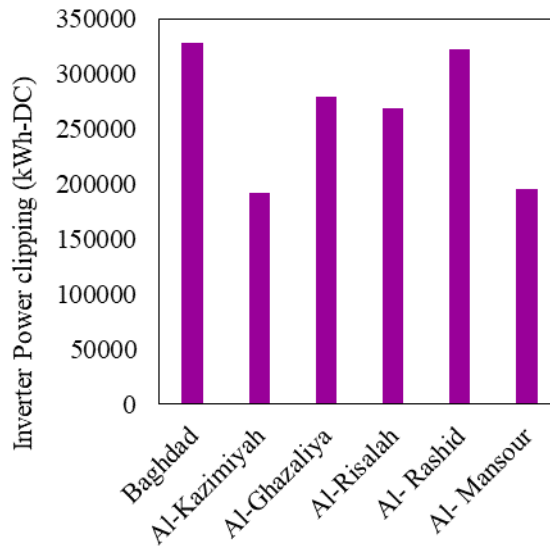


Fig.8.The amount of saturation losses of the inverter during one year.

The comparison between Figures 5 and 8 reveals that as the number of inverters increases (resulting in a decrease in the DC to AC conversion ratio from 1.21 to 1.06, the saturation losses of the inverter exhibit a significant decrease across all regions of the province. Specifically, the saturation losses have experienced a substantial reduction of approximately 60%. Seeing the difference between Figures 1 and 6 shows how important it is to lower inverter saturation losses. This shows that solar farms could improve their production capacity in a big way. The Al-Risalah Photovoltaic Power Plant is projected to have a 2.5% increase in its production capacity relative to its prior status.

Moreover, when the quantity of utilized inverters is increased to nine, the saturation loss of the inverters will be eliminated. The production capacity of solar fields is depicted in Figure 9 in this particular instance. A comparison between figures (1) and (9) reveals that the elimination of saturation losses in the inverter results in a 2.9% improvement in the production power of the Al-Risalah photovoltaic power plant.

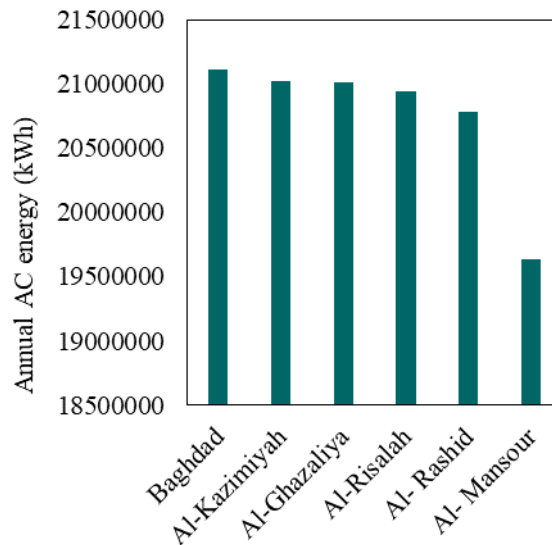


Fig. 9. AC energy produced by photovoltaic power plant in one year.

An additional observation that can be deduced from the findings presented in Figure 8 is the absence of a correlation between inverter saturation losses and the power plant's production rate, while a significant correlation is observed with the annual radiation curve of the specific geographical location. As illustrated in Figure 9, the power production in Baghdad surpasses that of Al-Rashid. The findings depicted in Figure 8 indicate that the saturation losses of the inverter in Al-Rashid exceed those of the inverter in Baghdad. It is important to acknowledge that the saturation loss of the inverter is independent of production quantity and instead correlates with the extent of divergence from the production standard.

A comparison is made between the production and saturation rates of inverters in the Baghdad and Al-Rashid regions in order to get a better sense of this problem. Figure 10 presents a comparison of the degree of divergence from the standard in production power between the two cities. Based on the data presented in Figure 10, it is evident that the level of deviation from the production standard in Al-Rashid exceeds that of Baghdad. Consequently, in comparison to the inverters at Baghdad Photovoltaic Power Plant, the inverters at Al-Rashid Power Plant will experience saturation more frequently.

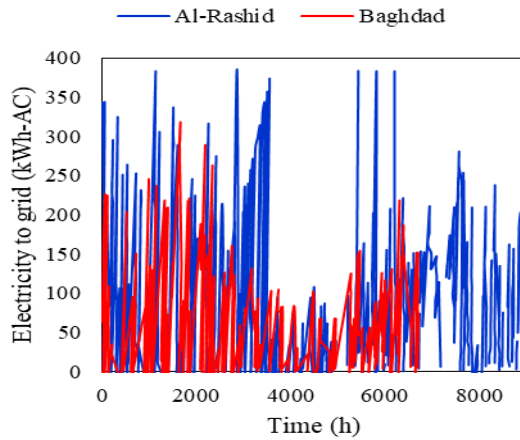


Fig.10. The amount of deviation from the production standard.

## 2. Conclusion

This article investigates the influence of inverter saturation losses on the overall efficiency of a solar power system. In order to fulfill the objective, meteorological data from cities located in Baghdad province, which is renowned for its significant capacity in solar energy production, has been obtained through the utilization of Metenorm. A simulation of a 10 MW photovoltaic farm has been conducted in SAM, taking into account the meteorological data specific to each region. The simulation incorporates a range of environmental and geographical variables, alongside losses associated with power plant components. The findings from the simulation demonstrate that the efficiency of the power plant is notably impacted by inverter saturation losses. The mitigation of these losses results in a significant enhancement of the output rate of the solar power plant. It is imperative to acknowledge that the aforementioned ratio exhibits variability across diverse geographical regions, while the saturation losses of the inverter are significantly influenced by the specific geographical location and its corresponding annual radiation pattern.

The findings of the study indicate a positive correlation between the level of inverter saturation losses and the hourly radiation of a certain region. There is a positive correlation between the magnitude of hourly radiation divergence from the annual average and the corresponding increase in saturation losses of the inverter. Furthermore, the sole feasible approach to mitigate inverter saturation losses entails augmenting the quantity of inverters employed in the power plant, hence resulting in an escalation of the capital expenditure.

## References

1. M. A. Destek and A. Sinha, "Renewable, non-renewable energy consumption, economic growth, trade openness and ecological footprint: Evidence from organisation for economic

- Co-operation and development countries," *Journal of cleaner production*, vol. 242, p. 118537, 2020.
2. F. Bélaïd and M. Youssef, "Environmental degradation, renewable and non-renewable electricity consumption, and economic growth: Assessing the evidence from Algeria," *Energy policy*, vol. 102, pp. 277-287, 2017.
  3. S. Saeidi, S.N. Enjedani, E.A. Behineh, K. Tehranian, and S. Jazayerifar, "Factors Affecting Public Transportation Use during Pandemic: An Integrated Approach of Technology Acceptance Model and Theory of Planned Behavior," *Tehnički glasnik* vol. 18, no. 3, p. 1-12, 2023
  4. K. O. Yoro and M. O. Daramola, "CO2 emission sources, greenhouse gases, and the global warming effect," in *Advances in carbon capture: Elsevier*, 2020, pp. 3-28.
  5. S. Khalili, E. Rantanen, D. Bogdanov, and C. Breyer, "Global transportation demand development with impacts on the energy demand and greenhouse gas emissions in a climate-constrained world," *Energies*, vol. 12, no. 20, p. 3870, 2019.
  6. T. M. Gür, "Carbon dioxide emissions, capture, storage and utilization: Review of materials, processes and technologies," *Progress in Energy and Combustion Science*, vol. 89, p. 100965, 2022.
  7. F. Belaïd, "Implications of poorly designed climate policy on energy poverty: Global reflections on the current surge in energy prices," *Energy Research & Social Science*, vol. 92, p. 102790, 2022.
  8. M. S. Nazir, Z. M. Ali, M. Bilal, H. M. Sohail, and H. M. Iqbal, "Environmental impacts and risk factors of renewable energy paradigm—a review," *Environmental Science and Pollution Research*, vol. 27, pp. 33516-33526, 2020.
  9. E. T. Sayed et al., "A critical review on environmental impacts of renewable energy systems and mitigation strategies: Wind, hydro, biomass and geothermal," *Science of the total environment*, vol. 766, p. 144505, 2021.
  10. W. U. K. Tareen et al., "The prospective non-conventional alternate and renewable energy sources in Pakistan—A focus on biomass energy for power generation, transportation, and industrial fuel," *Energies*, vol. 11, no. 9, p. 2431, 2018.
  11. R. M. Elavarasan, "The motivation for renewable energy and its comparison with other energy sources: A review," *European Journal of sustainable Development research*, vol. 3, no. 1, p. em0076, 2019.
  12. J. L. Holechek, H. M. Geli, M. N. Sawalhah, and R. Valdez, "A global assessment: can renewable energy replace fossil fuels by 2050?," *Sustainability*, vol. 14, no. 8, p. 4792, 2022.
  13. R. Lemm, R. Haymoz, A. Björnsen Gurung, V. Burg, T. Strebel, and O. Thees, "Replacing fossil fuels and nuclear power with renewable energy: Utopia or valid option? A Swiss case study of bioenergy," *Energies*, vol. 13, no. 8, p. 2051, 2020.
  14. D. Gielen et al., "Global energy transformation: a roadmap to 2050," 2019.
  15. M. Ram, A. Aghahosseini, and C. Breyer, "Job creation during the global energy transition towards 100% renewable power system by 2050," *Technological Forecasting and Social Change*, vol. 151, p. 119682, 2020.
  16. A. Sadiqa, A. Gulagi, and C. Breyer, "Energy transition roadmap towards 100% renewable energy and role of storage technologies for Pakistan by 2050," *Energy*, vol. 147, pp. 518-533, 2018.
  17. S. Sharma, S. Agarwal, and A. Jain, "Significance of hydrogen as economic and environmentally friendly fuel," *Energies*, vol. 14, no. 21, p. 7389, 2021.
  18. W. S. Ebhota and T.-C. Jen, "Fossil fuels environmental challenges and the role of solar photovoltaic technology advances in fast tracking hybrid renewable energy system," *International Journal of Precision Engineering and Manufacturing-Green Technology*, vol.

- 7, pp. 97-117, 2020.
19. P. A. Sanchez, *Properties and Management of Soils in the Tropics*. Cambridge University Press, 2019.
  20. W. G. Whitford and B. D. Duval, *Ecology of desert systems*. Academic Press, 2019.
  21. K. A. Horowitz, B. Palmintier, B. Mather, and P. Denholm, "Distribution system costs associated with the deployment of photovoltaic systems," *Renewable and Sustainable Energy Reviews*, vol. 90, pp. 420-433, 2018.
  22. M. Kumar, H. M. Niyaz, and R. Gupta, "Challenges and opportunities towards the development of floating photovoltaic systems," *Solar Energy Materials and Solar Cells*, vol. 233, p. 111408, 2021.
  23. D. Horváth and R. Z. Szabó, "Evolution of photovoltaic business models: Overcoming the main barriers of distributed energy deployment," *Renewable and Sustainable Energy Reviews*, vol. 90, pp. 623-635, 2018.
  24. L. Dias, J. P. Gouveia, P. Lourenço, and J. Seixas, "Interplay between the potential of photovoltaic systems and agricultural land use," *Land use policy*, vol. 81, pp. 725-735, 2019.
  25. A. Louwen and W. Van Sark, "Photovoltaic solar energy," in *Technological learning in the transition to a low-carbon energy system*: Elsevier, 2020, pp. 65-86.
  26. Jamalpour, H., & Yaghoobi-Derabi, J. (2022). Cultural memory and neuro-critical reading of Ian McEwan's atonement. *Revista de Investigaciones Universidad del Quindío*, 34(S2), 436-442.
  27. Zarepour, G., & Javanshir, I. (2021). Semi-Analytical Study of Fluid-Induced Nonlinear Vibrations in Viscoelastic Beams with Standard Linear Solid Model Using Multiple Time Scales Method. *Amirkabir Journal of Mechanical Engineering*, 53(10), 5105-5122.
  28. Jamalpour, H., & Verma, A. (2022). *Introduction to Psychoanalysis: A New Perspective on Linguistics and Psychoanalysis*, Vol. 1, Rose Publication PTY LTD, Melbourne, Australia.
  29. Javanshir, I., Javanshir, N., Barmaki, R., & Mahmoodi, M. (2015). Modeling of the fluid-induced vibrations in sliding gate dams. *Journal of Vibroengineering*, 17(1), 478-486.
  30. Jamalpour, H., & Derabi, J. Y. (2023). Aesthetic Experience, Neurology and Cultural Memory. *Passagens: Revista Internacional de História Política e Cultura Jurídica*, vol. `5, no. 2, pp. 340-348, <https://doi.org/10.15175/1984-2503-202315208>
  31. G. Kucur, M. R. Tur, R. Bayindir, H. Shahinzadeh, and G. B. Gharehpetian, "A Review of Emerging Cutting-Edge Energy Storage Technologies for Smart Grids Purposes," in *2022 9th Iranian Conference on Renewable Energy & Distributed Generation (ICREDG), 2022: IEEE*, pp. 1-11.
  32. R. Khan et al., "Energy sustainability–survey on technology and control of microgrid, smart grid and virtual power plant," *IEEE Access*, vol. 9, pp. 104663-104694, 2021.
  33. J. Oyekale, M. Petrollese, V. Tola, and G. Cau, "Impacts of renewable energy resources on effectiveness of grid-integrated systems: Succinct review of current challenges and potential solution strategies," *Energies*, vol. 13, no. 18, p. 4856, 2020.
  34. L. Idoko, O. Anaya-Lara, and A. McDonald, "Enhancing PV modules efficiency and power output using multi-concept cooling technique," *Energy Reports*, vol. 4, pp. 357-369, 2018.
  35. A. Al-Bashir, M. Al-Dweri, A. Al-Ghandoor, B. Hammad, and W. Al-Kouz, "Analysis of effects of solar irradiance, cell temperature and wind speed on photovoltaic systems performance," *International journal of energy economics and policy*, vol. 10, no. 1, p. 353, 2020.
  36. R. Rotar, S. L. Jurj, F. Opritoiu, and M. Vladutiu, "Position optimization method for a solar tracking device using the cast-shadow principle," in *2018 IEEE 24th International Symposium for Design and Technology in Electronic Packaging(SIITME), 2018: IEEE*, pp. 61-70.